Chapter 1. Global agroclimatic patterns

1.1 Introduction to CropWatch agroclimatic indicators (CWAIs)

This bulletin describes environmental and crop conditions over the period from January 2021 to April 2021, JFMA, referred to as "reporting period". In this chapter, we focus on 65 spatial "Mapping and Reporting Units"(MRU) which cover the globe, but CWAIs are averages of climatic variables over agricultural areas only inside each MRU. For instance, in the "Sahara to Afghan desert" MRU, only the Nile valley and other cropped areas are considered. MRUs are listed in annex C and serve the purpose of identifying global climatic patterns. Refer to Annex A for definitions and to table A.1 for 2021 JFMA numeric values of CWAIs by MRU. Although they are expressed in the same units as the corresponding climatological variables, CWAIs are spatial averages limited to agricultural land and weighted by the agricultural production potential inside each area.

We also stress that the reference period, referred to as "average" in this bulletin covers the 15-year period from 2006 to 2020. Although departures from the 2005-2019 are not anomalies (which, strictly, refer to a "normal period" of 30 years), we nevertheless use that terminology. The specific reason why CropWatch refers to the most recent 15 years is our focus on agriculture, as already mentioned in the previous paragraph. 15 years is deemed an acceptable compromise between climatological significance and agricultural significance: agriculture responds much faster to persistent climate variability than 30 years, which is a full generation. For "biological" (agronomic) indicators used in subsequent chapters we adopt an even shorter reference period of 5 years (i.e. 2016-2020) but the BIOMSS indicator is nevertheless compared against the longer 15YA (fifteen-year average). This makes provision for the fast response of markets to changes in supply but also to the fact that in spite of the long warming trend, some recent years (e.g. 2008 or 2010-13) were below the trend.

Correlations between variables (RAIN, TEMP, RADPAR and BIOMSS) at MRU scale derive directly from climatology. For instance, the positive correlation between rainfall and temperature results from high rainfall in equatorial, i.e. in warm areas.

Considering the size of the areas covered in this section, even small departures may have dramatic effects on vegetation and agriculture due to the within-zone spatial variability of weather.

1.2 Global overview

Weather conditions during this monitoring period were influenced by a La Niña conditions and a break-down of the polar vortex. La Niña officially ended in March 2021. It brought wetter conditions to eastern Australia and drier conditions to equatorial Africa. The weakening and break-down of the polar vortex caused cold spells mainly in the USA and Europe. Its break-down in early February caused freezing conditions as far south as Texas in the USA for several days.

Figure 1.1 shows unweighted averages of the CropWatch Agroclimatic Indicators, i.e. the arithmetic means of all 65 MRUs, which are relatively close to average. CWAIs are computed only over agricultural areas, and they display a relatively average situation, globally.

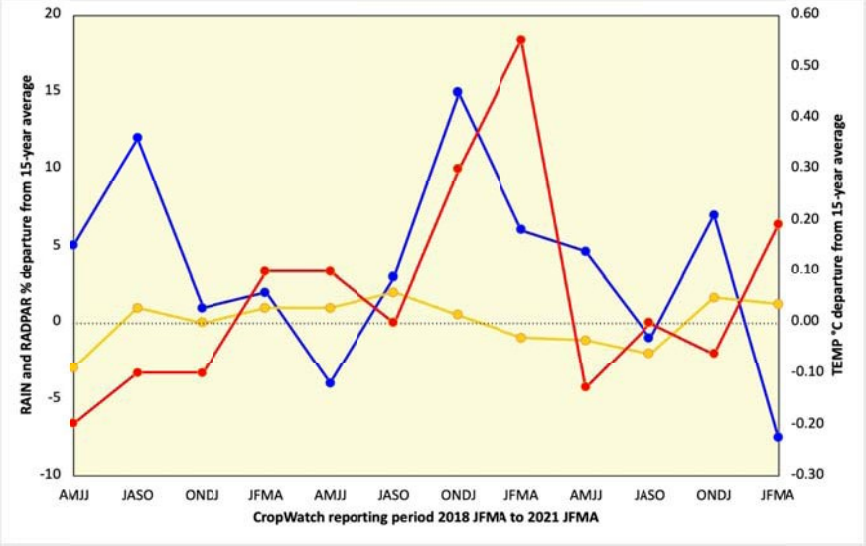

Figure 1.1 global departure from recent 15 year average of the RAIN, TEMP and RADPAR indicators since 2018 JASO period (average of 65 MRUs, unweighted)

1.3 Rainfall (Figure 1.2)

Below average rainfall conditions persisted in the west of North America, from Alaska down to Mexico. The most severe rainfall deficit, with rainfall being more than 30% below average, was observed for Mexico, large parts of Brazil stretching from the Pantanal to Mato Grosso and the North East. The Middle East, Central Asia, Northern South Asia and Tibet also experienced a severe rainfall deficit. The Amazon Basin, Southern Chile, the northeast of the USA, South-Eastern China, as well as West- and Central Africa, including Madagascar experienced a rainfall deficit by 10-30%. These rainfall deficits are especially problematic when they occur during the periods in which most precipitation falls. In this period, this was the case for the West Coast of the USA, the Amazon Basin including most of Brazil, Southern Africa, Madagascar, the Middle East and Central Asia. Western Russia and the Ukraine, as well as Eastern Siberia, North China, the Korean Peninsula and Japan, as well as Australia received above average precipitation. Abundant rainfall helped Australia overcome the severe drought that had occurred in 2020.

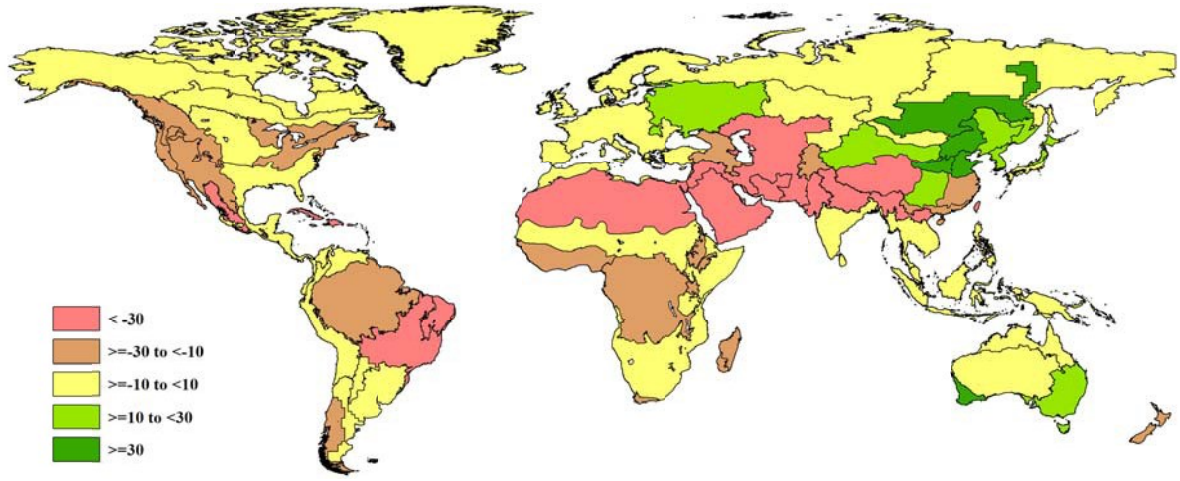

Figure 1.2 Global map of rainfall anomaly (as indicated by the RAIN indicator) by CropWatch Mapping and Reporting Unit: departure of January to April 2021 total from 2006-2020 average (15YA), in percent.

1.4 Temperatures (Figure 1.3)

Most of the regions experienced normal temperatures, i.e., the averages did not depart by more than +/- 0.5□C from the 15YA. Cooler than average temperatures in the range of -1.5 to -0.5□C were observed for the southeast of the USA, most of Europe, except the south and very north, East Africa and Australia. Above average temperatures in the range of +0.5 to +1.5 □C were observed for Brazil, Middle East, Central Asia and East Asia, including China, South-east Siberia, Korea and Japan. Only a couple of relatively small regions experienced above average temperatures exceeding +1.5□C. These areas were a belt stretching across Canada from the Western Prairies to the East Coast and Eastern Japan.

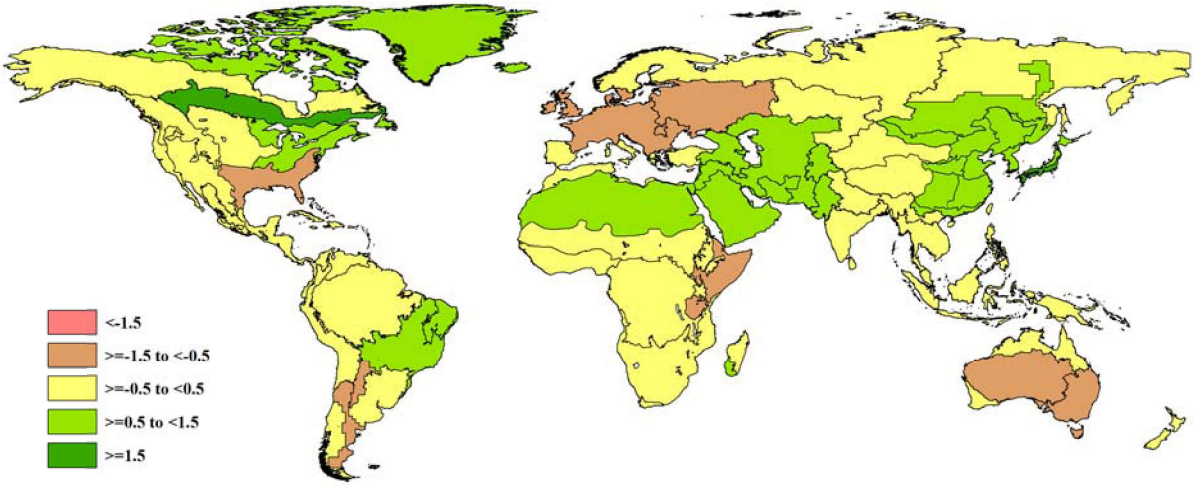

Figure 1.3 Global map of temperature anomaly (as indicated by the TEMP indicator) by CropWatch Mapping and Reporting Unit: departure of January to April 2021 average from 2006-2020 average (15YA), in ℃.

1.5 RADPAR (Figure 1.4)

The west of north America experienced much above average solar radiation, i.e., by more than 3%, together with Madagascar. The entire west of the USA, most of Europe, the Middle East, Central Asia and the Indonesia Archipelago experienced above average solar radiation as well. Below average solar radiation was recorded for the central and eastern part of the USA, most of South America except for Central Brazil, Africa south of the Sahara, Russia and North and Eastern China as well as Australia. The deficits were largest for Australia and Russia.

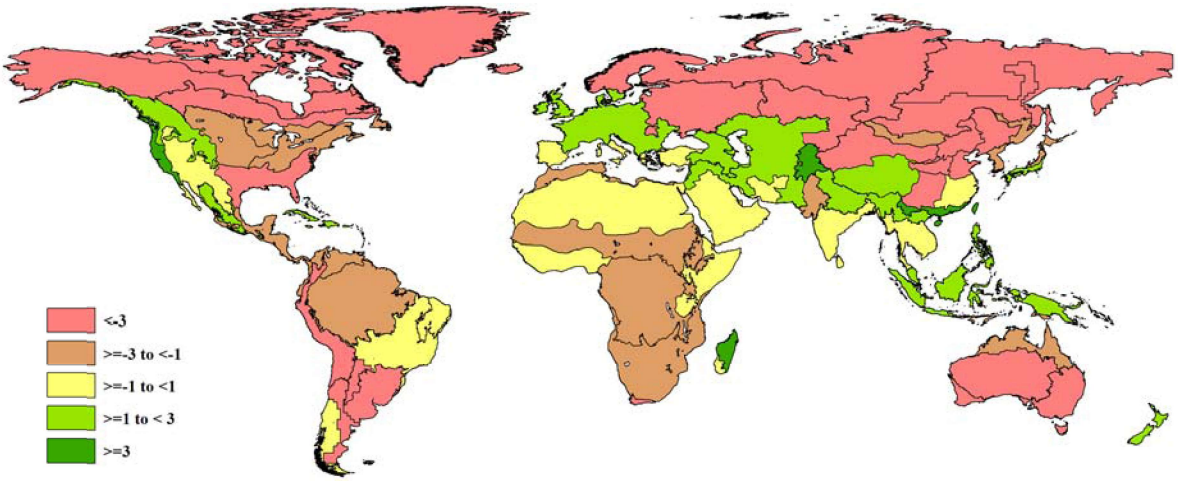

Figure 1.4 Global map of photosynthetically active radiation anomaly (as indicated by the RADPAR indicator) by CropWatch Mapping and Reporting Unit: departure of January to April 2021 total from 2006-2020 average (15YA), in percent.

1.5 BIOMSS (Figure 1.5)

Estimated biomass, which is calculated as a function of temperature, rainfall and solar radiation, showed a relatively large negative departure by more than -5% for Africa, Central Asia, South and Southeast Asia, Europe, Russia, and southern China. Potential biomass was also significantly lower than average in the western United States and central to northeastern Brazil. Northern China, the Korean Peninsula, Japan, and southwestern Australia benefited from abundant precipitation and had significantly above-average potential biomass.

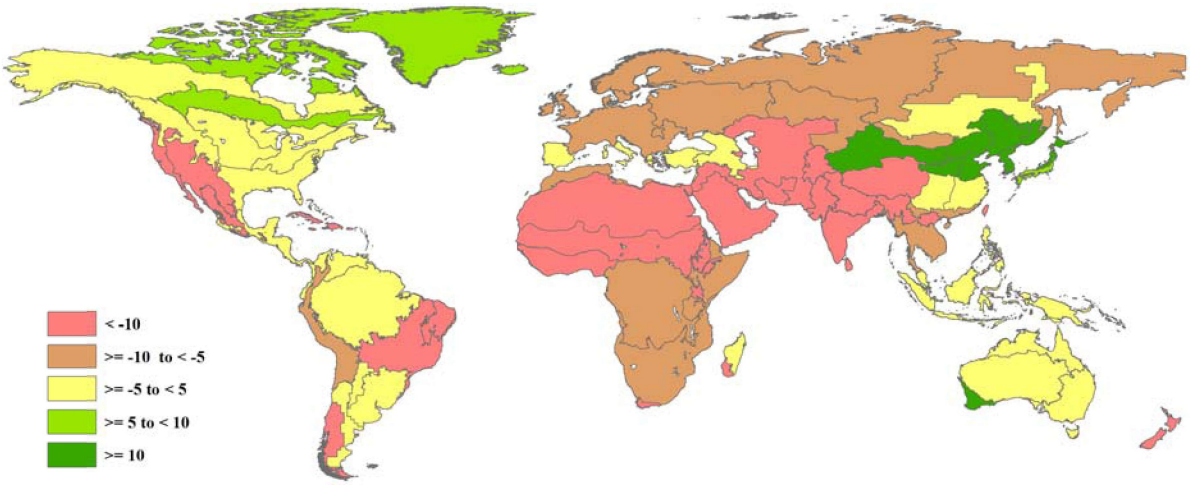

Figure 1.5 Global map of biomass accumulation (as indicated by the BIOMSS indicator) by CropWatch Mapping and Reporting Unit: departure of January to April 2021 total from 2006-2020 average (15YA), in percent.